STRAIN RATE EFFECTS IN METALLIC CELLULAR MATERIALS

Sungsoo Lee, Francois Barthelat and Horacio D. Espinosa
Northwestern University
2145 Sheridan Rd.
Evanston, IL 60208-3111
U.S.A.

ABSTRACT

The high strain rate behavior of two cellular materials was investigated using a quasi-static loading stage and a Kolsky bar apparatus. The yield stress of these core materials under dynamic loading was found higher than in quasi-static loading. However, the plateau stress after yielding is not so sensitive to strain rate. For Aluminum foam materials, the deformation was more localized for quasi-static loading than under dynamic loading, where the collapse of cells was more distributed. Several failure modes were found in topologically structured cellular core (tetragonal truss), and these modes are strongly dependent on initial defects.

INTRODUCTION

Motivated by recent advances in materials science, manufacturing, and optimization, attention is being focused on metallic sandwich panels for various applications such as automotive, locomotive and aerospace [1]. Sandwich plates with solid face sheets and cellular core materials have low densities, and have been found highly efficient in absorbing mechanical impulse where weight reduction is needed.

Many researchers have been studying the strain rate dependence of strength and energy absorption of aluminium alloy foams [2-4]. However no quantitative result was reported about the different failure mechanisms. Tam and Calladine [5], and Reid and co-workers [6-9] observed an increase of strength for higher strain rates. They proposed micro-inertia or shock wave propagation effects as main contributors to this rate effect. However they did not directly observe failure mechanisms in-situ.

Previous studies on the behavior of cellular materials have been mainly performed on foam materials with randomly shaped and distributed cells. Truss cores with tetragonal topologies were theoretically studied by Wicks and Hutchinson[10], Deshpande and Fleck [11], Wallach and Gibson [12, 13], Evans et al. [14], and Deshpande et al. [15]. They were predicted to offer the best combination of compressive strength and low weight. Experimental measurements and numerical simulations were performed to validate this prediction by Chiras et al. [16].
As these truss cores where studied theoretically and numerically, few experimental data was reported, and the experiments performed were limited to quasi-static loading.

In this paper, the high strain rate behavior of an Aluminum foam material and a 304 stainless steel tetragonal truss core material was investigated. Comparing results from quasi-static loading stage and the Kolsky bar system, strain rate effects in the cellular materials were directly observed. A unique technique was used, where specimen displacements and deformations are measured optically in real time and correlated to applied stress history. To capture the history of specimen deformation optically, a 3-CCD video camera with a macro zoom lens was employed for quasi-static cases, and an ultra-high-speed 8-CCD camera with a long distance microscope was utilized for dynamic cases. Digital image correlation (DIC) was employed to obtain deformation fields in the specimen, and to examine local deformations and the sequence of material instabilities and failure. Using this technique, it was possible to discriminate the different failure mechanisms under quasi-static and dynamic loading.

EXPERIMENTAL PROCEDURE

Compression tests were performed on the aluminium foam and on the stainless steel truss core material under quasi-static and dynamic loadings. Fig. 1 shows the quasi-static experimental setup. The loading stage is equipped with control unit, load cell, LVDT, and signal processing units which are connected to a PC. The optical measurement is made by a 3-CCD video camera equipped with a macro zoom lens, and the camera is connected to a video capture board in the PC. The program records all the inputs simultaneously and ensures that they are synchronized. After the test is done, frames are extracted from the recorded movie and processed by DIC to get the deformation fields in the specimen. By measuring the deformations directly on the specimen, complications due to frame compliance were alleviated.

Proceedings of the 2003 SEM Annual Conference and Exposition on Experimental and Applied Mechanics, June 2-4, Charlotte, North Carolina, Session 37, Paper 188, 2003.

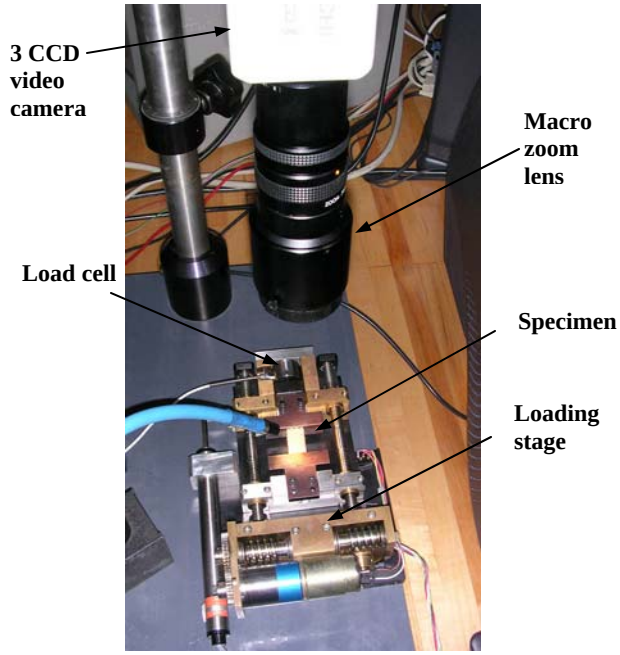

Figure 1. Experimental setup of quasi-static loading and measurement

For experiments in dynamic conditions, a stored-energy type Kolsky bar apparatus was used (Fig. 2). The apparatus is mainly composed of two 1" diameter aluminum bars mounted on linear bearings. The specimen is placed between the bars. To store the energy, the incident aluminum bar is clamped and a compressive load is applied using a hydraulic actuator. Upon release of the clamp, a compressive stress wave travels down the bar, into the specimen and the transmitted bar. Strain gage stations at different locations on the bars are used to record incident, reflected, and transmitted pulses. The velocity at a point can be obtained by:

$$\dot{u}(x,t) = \frac{4c_L F(x,t)}{\pi D^2 E_{Al}} \qquad (1)$$

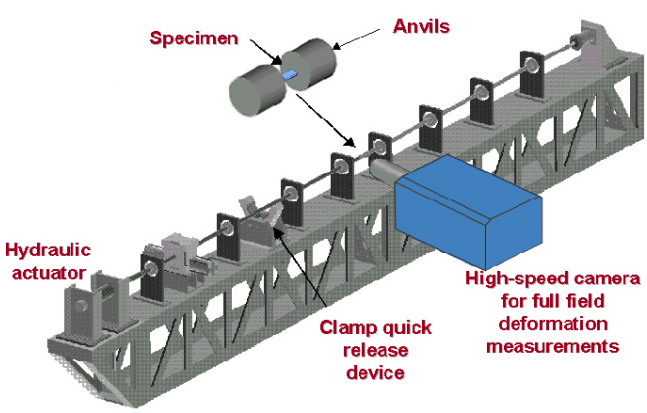

Figure 2. Experimental setup of dynamic tests and measurement

where c_L is the sound speed in aluminum, F is the load, D is the bar diameter, and E_{Al} is the Young's modulus of aluminium. From Eq. (1), we can calculate the compression of the specimen:

$$\Delta u(t) = \frac{8c_L}{\pi D^2 E_{Al}} \int_0^t (F_i(0,t) - F_t(0,t))dt \qquad (2)$$

where x=0 indicates the interface between the incident bar and the specimen, subscript i denotes incident pulse, and subscript t denotes transmitted pulse. In addition to the integration method, the incident pulse triggers a high-speed camera, which captures up to 8 snapshots of the specimen during the dynamic test. The full range of displacement field is obtained by employing DIC technique. All the pulses and video images are synchronized and transferred to PC to process the data.

The Aluminum foam had open cell architecture with 8% relative density. The specimen was 25mm x 15mm x 15mm (Fig. 3). Truss core materials (Fig. 4) were also tested. Unit cells were cut from a sheet of the material, using abrasive saw at high RPM and very low feeding rate to minimize damage to the truss members. Detailed information on the truss core samples can be found in Table 1.

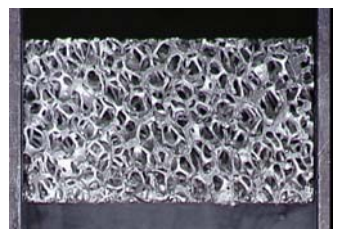

Figure 3. Al foam specimen

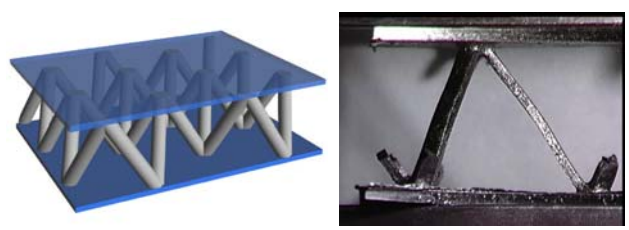

Figure 4. Schematic of tetragonal truss core material sandwiched by two facesheets and its unit cell

Table 1. Properties of tetragonal truss core material and the specimen

Overall	Material	304 stainless steel
	Relative Density	2%
	Thickness	10.9 mm
Truss member	Length	11.4 mm
	Width	1.2 mm
	Thickness	0.55 mm
Facesheets	Thickness	0.7 mm

RESULTS AND DISCUSSION

Fig. 5 shows curves of nominal stress versus nominal strain for quasi-static and dynamic compression tests on the Aluminum foam material. The strain rate in quasi-static case was 2.5 x 10^{-3} s^{-1} and that of dynamic loading was 120 s^{-1}. All the curves show an initial linear elastic region followed by a plateau region. Although the stress in dynamic loading is a slightly higher than that of quasi-static, the plateau stress in dynamic experiments #2 is similar to those of quasi-static cases.

Fig. 6 shows 8 images captured by the high-speed camera. The shots are taken at an interval of 100 μs. The sequence of compression clearly shows the collapse of some cells.

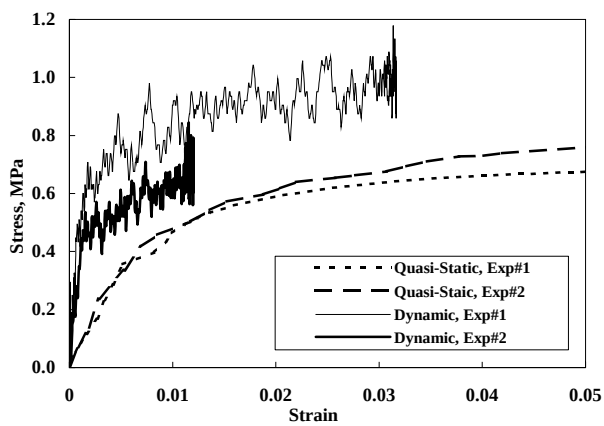

Figure 5. Comparison between quasi-static and dynamic compression of Al foam

To understand the different failure mechanisms between quasi-static and dynamic cases, and compare them quantitatively, digital image correlation technique was used. Fig. 7 shows full range deformation fields in the specimens computed using digital image correlation techniques for both quasi-static and dynamic loadings. The image shown corresponds to the same level of overall strain, marked by dotted lines on the stress-strain curve. The results show the localized deformations in dynamic case are spread along the whole specimen, while in quasi-static case the deformations are more concentrated, in a line running across the axis of the specimen.

The large deformations involved in cell crushing imply significant motion of material in buckling cell walls and ligaments. In dynamic mode, this motion implies micro-inertia effect, and the result is that it takes more force to crush the cells. The strains are therefore more spatially distributed than for the quasi-static case.

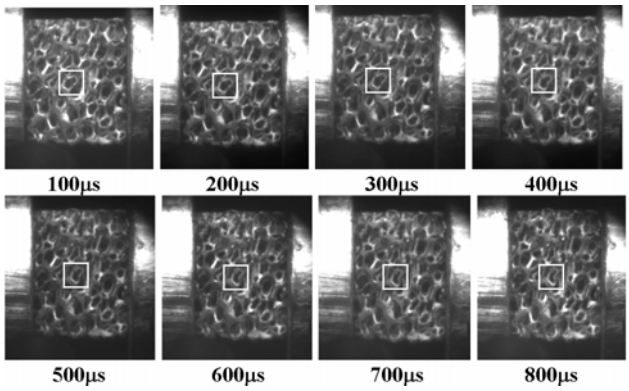

Figure 6. Sequence of dynamic compression and collapse of cells captured by high speed photography

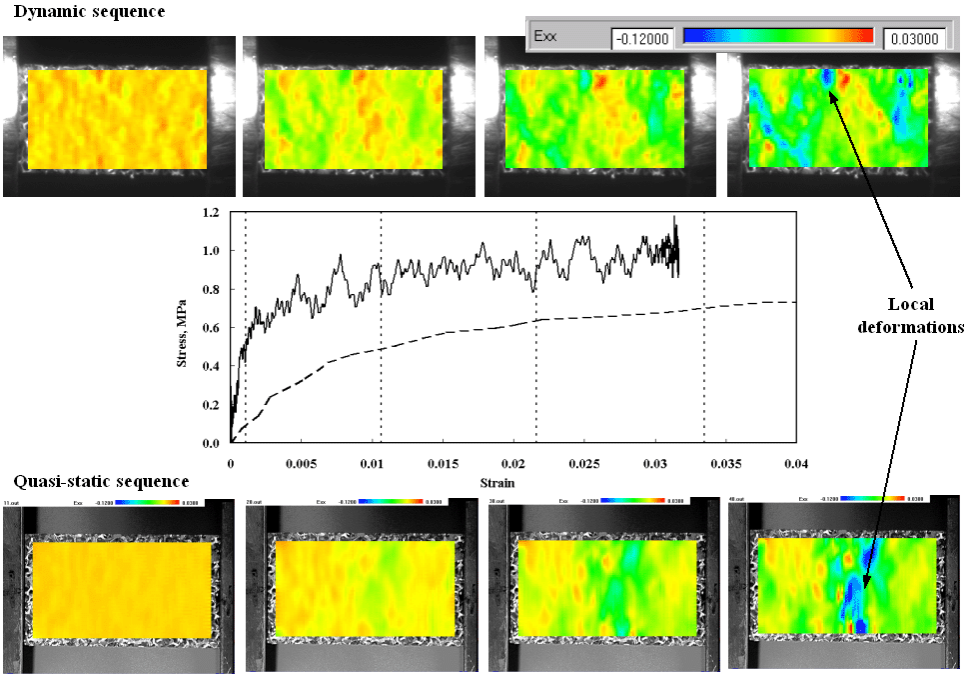

Figure 7. Deformation fields in quasi-static and dynamic loading conditions computed by digital image correlation technique

Fig. 8 shows curves of load versus relative displacement of stainless steel tetragonal truss core specimens under quasi-static and dynamic loading. The curves show an initial linear region until the load reaches a peak value, where the material becomes unstable. The load then decreases to what seems to be a steady state value. Nominal stresses and strains can be calculated by the load and relative displacement. In quasi-static loading, the relative velocity is $7x10^{-6}$ $m.s^{-1}$, corresponding to a strain rate of $7.37x10^{-4}$ s^{-1}. The dynamic experiments were performed at a relative velocity of 2.5 $m.s^{-1}$ and a strain rate of 263 s^{-1}. Based on beam theory calculations the elastic stiffness of the core material was predicted to be 30.4 $kN.mm^{-1}$. The experimental results are in good agreement with this prediction as the linear region of initial curves yields 30 $kN.mm^{-1}$ for both cases. The Quasi-static peak load is 320 N, almost half of the peak load in dynamic loading (600 N). However, the plateau load after yield is almost the same in both cases.

In three dynamic experiments, the truss cores experienced three different failure modes as shown in Fig. 9. Careful inspections of initial slight bending in the truss members and of the pictures revealed that the buckling modes seem dependent on the initial defects. Nevertheless, the load response does not seem to be affected by the buckling mode.

Another interesting feature of this material is subsequent stiffening leading to a further increase in energy absorption. Fig. 10 shows load compression curves in quasi-static mode for tests pursued at larger compression levels. The curves show three sudden increase in stiffness, corresponding to the three buckled legs entering in contact with the upper face sheet. The load becomes subsequently higher than the initial peak load.

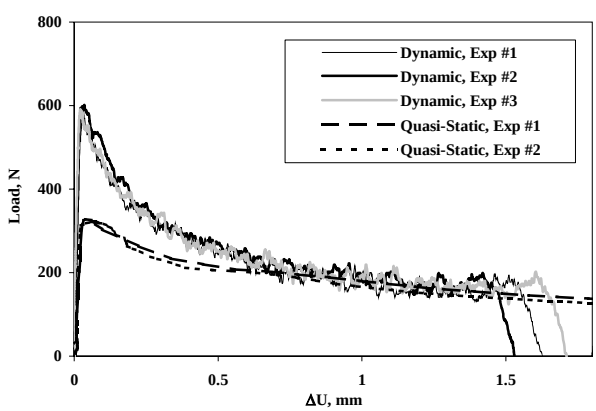

Figure 8. Comparison between quasi-static and dynamic experiments of stainless steel tetragonal truss core material

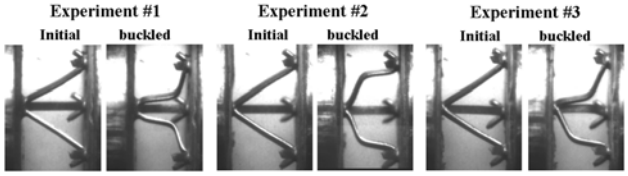

Figure 9. Three different failure modes shown in tetragonal truss core

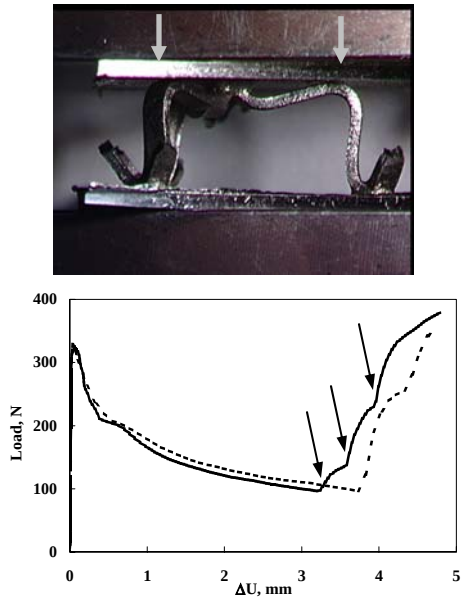

Figure 10. Stiffening of the system in plastic region of tetragonal truss core material under quasi-static load

CONCLUSION AND FUTURE WORK

The mechanical behavior of the cellular metallic materials, subjected to dynamic loading conditions, was investigated. Aluminum foams and 304 stainless steel tetragonal truss core materials were tested under quasi-static and dynamic compressive loads. Using advanced optical measurement technique, failure modes in quasi-static and dynamic conditions were captured simultaneously with histories of load and displacement.

In-situ compression testing and digital image correlations are robust methods to determine local deformations in the specimens. For the tests of foams, a crushing band was clearly seen in quasi-static loading in comparison with dynamic case. The peak stress in dynamic loading is higher than in quasi-static but the plateau stress is in the same order.

Further study will investigate the effect of the relative density on the peak stress and energy absorption of the material. The results will then be utilized to determine the optimal design for various applications. Since various different topologies are under investigation for theoretical, computational, and statically experimental studies, dynamic experiments on the samples of the different topologies will be performed.

ACKNOWLEDGEMENTS

This work was sponsored by the Office of Naval Research under Award No. 123163-02-N00014-02-1-0700. Special thanks are due to Professors A. Evans and F. Zok, and Dr. H. Rathbun at University of California at Santa Barbara, and Professor H. Wadley, Dr. K. Dharmasena, and Dr. D.T. Queheillalt at University of Virginia for their aid in fabrication of samples and helpful discussions.

REFERENCES

[1] Gibson, L.J., and Ashby, M.F., Cellular Solids, Structure and Properties, 2nd ed., Cambridge University Press, Cambridge, UK, 1997.

[2] Dannemann, K., and Lankford Jr., J., High Strain Rate Compression of Closed-Cell Aluminium Foams, Materials Science and Engineering, A293, pp. 157-164, 2000.

[3] Deshpande, V.S., and Fleck, N.A., High Strain Rate Compressive Behavior of Aluminium Alloy Foams, International Journal of Impact Engineering, 24, pp. 277-298, 2000.

[4] Yi, F., Zhu, Z., Hu, S., Yi, P., He, L., and Ning, T., Dynamic Compressive Behavior of Aluminium Alloy Foams, Journal of Materials Science Letters, 20, pp. 1667-1668, 2001.

[5] Tam, L.L., and Calladine, C.R., Inertia and Strain-Rate Effects in a Simple Plate-Structure under Impact Loading, International Journal of Impact Engineering, 11(3), pp. 349-377, 1991.

[6] Su, X.Y., Yu, T.X., and Reid, S.R., Inertia-Sensitive Impact Energy-Absorbing Structures. Part I: Effects of Inertia and Elasticity, International Journal of Impact Engineering, 16(4), pp. 651-672, 1995.

[7] Su, X.Y., Yu, T.X., and Reid, S.R., Inertia-Sensitive Impact Energy-Absorbing Structures. Part II: Effects of Strain Rate, International Journal of Impact Engineering, 16(4), pp. 673-689, 1995.

[8] Reid, S.R., and Peng, C., Dynamic Uniaxial Crushing of Wood, International Journal of Impact Engineering, 19, pp. 531-570, 1997.

[9] Tan, P.J., Harrigan, J.J., and Reid, S.R., Inertia Effects in Uniaxial Dynamic Compression of a Closed Cell Aluminium Alloy Foam, Materials Science and Technology, 18, pp. 480-488, 2002.

[10] Wicks, N., and Hutchinson, J.W., Optimal Truss Plates, International Journal of Solids and Structures, 38 (30-31), pp. 5165-5183, 2001.

[11] Deshpande, V.S., and Fleck, N.A., Collapse of Truss Core Sandwich Beams in 3-Point Bending, International Journal of Solids and Structures, 38 (36-37), pp. 6275-6305, 2001.

[12] Wallach, J.C., and Gibson, L.J., Mechanical Behavior of a Three-Dimensional Truss Material, International Journal of Solids and Structures, 38 (40-41), pp. 7181-7196, 2001.

[13] Wallach, J.C., and Gibson, L.J., Defect Sensitivity of a 3D Truss Material, Scripta Materialia, 45 (6), pp. 639-644, 2001.

[14] Evans, A.G., Hutchinson, J.W., Fleck, N.A., Ashby, M.F., and Wadley, H.N.G., The Topological Design of Multifunctional Cellular Metals, Progress in Materials Science, 46 (3-4), pp. 309-327, 2001.

[15] Deshpande, V.S., Fleck, N.A., and Ashby, M.F., Effective Properties of the Octet-Truss Lattice Material, Journal of the Mechanics and Physics of Solids, 49 (8), pp. 1747-1769, 2001.

[16] Chiras, S., Mumm, D.R., Evans, A.G., Wicks, N., Hutchinson, J.W., Dharmasena, K., Wadley, H.N.G., and Fichter, S., The Structural Performance of Near-Optimized Truss Core Panels, International Journal of Solids and Structures, 39 (15), pp. 4093-4115, 2002.